Electronic Supplementary Material (ESI) for ChemComm.
This journal is © The Royal Society of Chemistry 2014

Supporting Information

A microporous six-fold interpenetrated hydrogen-bonded organic framework with for highly selective separation of C_2H_4/C_2H_6

Peng Li,[a] Yabing He,[a] Hadi D. Arman,[a] Rajamani Krishna,[b] Hailong Wang,[a] Linhong Weng,[c] Banglin Chen*[a,d]

[a] *Department of Chemistry, University of Texas at San Antonio, One UTSA Circle, San Antonio, Texas 78249-0698, United States Fax: (+1)-210-458-7428; E-mail: banglin.chen@utsa.edu*

[b] *Van 't Hoff Institute for Molecular Sciences, University of Amsterdam, Science Park 904, 1098 XH Amsterdam, The Netherlands*

[c] *Department of Chemistry, Fudan University, Shanghai, 200433, People's Republic of China.*

[d] *Department of Chemistry, Faculty of Science, King Abdulaziz University, Jeddah 22254, Saudi Arabia*

1. General remark

Thermogravimetric analyses (TGA) were performed with a Shimadzu TGA-50 analyzer under nitrogen atmosphere with a heating rate of 3 ^{o}C min^{-1}. Powder X-ray diffraction (PXRD) patterns were recorded by a Rigaku Ultima IV diffractometer operated at 40 kV and 44 mA with a scan rate of 1.0 deg min^{-1}. FTIR spectra were performed at a Bruke Vector 22 infrared spectrometer at room temperature. ^{1}H NMR and ^{13}C NMR spectra were obtained using a Varian Mercury 300 MHz spectrometer at room temperature. Tetramethylsilane (TMS) and deuterated solvents ($CDCl_3$, δ = 77.0 ppm; DMSO-d_6, δ = 39.5 ppm) were used as internal standards in ^{1}H NMR and ^{13}C NMR experiments, respectively. The elemental analyses were performed with Perkin–Elmer 240 CHN analyzers from Galbraith Laboratories, Knoxville. A Micromeritics ASAP 2020 surface area analyzer was used to measure gas adsorption isotherms. To have a guest-free framework, the fresh sample was exchanged with diethyl ether for at least 3 times, filtered and dried at room temperature for 24 hrs prior to measurements. The crystallographic measurement was performed on a Rigaku X-ray diffractometer system equipped with a Mo-target X-ray tube (λ = 0.71073 Å) at 193 (2) K. The structure was solved by direct methods and refined by full matrix least-squares methods with the SHELX-97 program package. The solvent molecules in as-synthesized HOF crystal are in highly disordered. The SQUEEZE subroutine of the PLATON software suit was used to remove the scattering from the highly disordered guest molecules.

2. General procedure of synthesis of organic building block and HOF-4

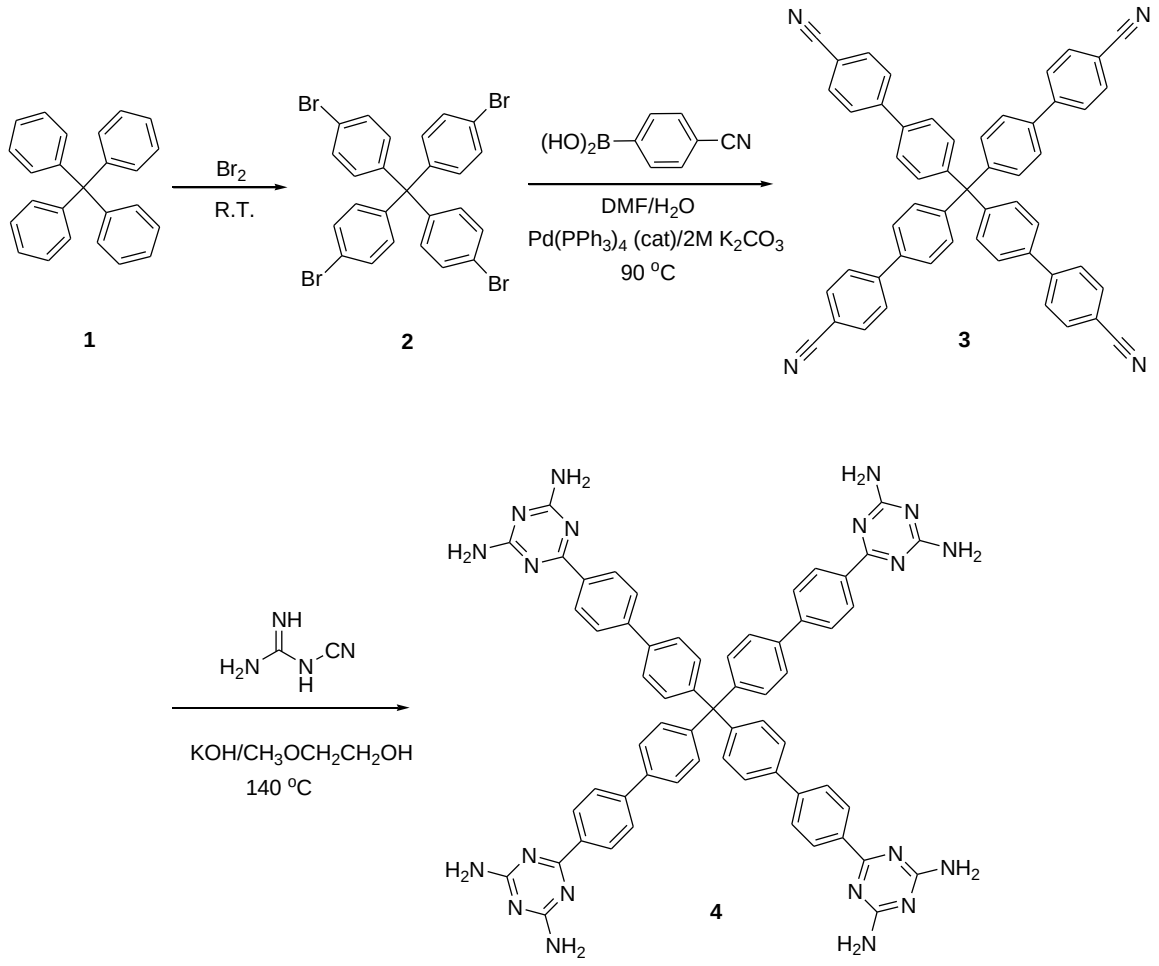

Scheme S1. Synthesis and characterization of the organic building block **4**

Tetrakis(4-bromophenyl)methane (2): Bromine (10.00 mL, 194.61 mmol) was added slowly to tetraphenylmethane (**1**) (9.00 g, 28.09 mmol) with continuous stirring. The resulting slurry was stirred for an additional 5 h and then poured into ethanol (200 mL) which was cooled to -78 ^{o}C. The precipitated solid was filtered, washed with saturated aqueous NaHSO3 solution (80 mL 3) and dried at 60 oC under vacuum to give a white solid (17.52 g, 27.55 mmol) in 98% yield. ^{1}H NMR (DMSO-*d*6, 300.0 MHz) δ (ppm): 7.51 (d, J = 8.7 Hz, 8H), 6.99 (d, J = 8.7 Hz, 8H); ^{13}C

NMR (DMSO-*d*6, 75.4 MHz) δ (ppm): 144.34, 132.20, 130.93, 119.81, 63.17; FTIR (neat, cm^{-1}): 1569, 1479, 1079, 1009, 950, 914, 835, 810, 752, 729, 679.

Tetrakis(4'-cyano-[1,1'-biphenyl]-4-yl)methane (3): A mixture of 4-cyanophenylboronic acid (17.63 g, 120.01 mmol) and tetrakis(4-bromophenyl)methane (13.63 g, 21.43 mmol) in DMF (80 mL), H_2O (40 mL), and aqueous K_2CO_3 (40 mL, 2M) was degassed by allowing N_2 to bubble through it. $Pd(PPh_3)_4$ (1150 mg, 1.00 mmol) was then added, and the mixture was degassed again. The mixture was heated at 90 ^oC for 48 h under N_2 and was exposed to air for 1 h to oxidize the catalyst. After removal of solvent under vacumn, the residue was extracted with CH_2Cl_2 (100 mL×3) and aqueous sodium ethylenediaminetetraacetate (50 mL×3) and brine (50 mL). The organic layer was separated and dried over anhydrous magnesium sulfate, filtered and evaporated to dryness. The resulting residue was purified by silica gel column chromatography with $CHCl_3$ as eluent to give a white solid (8.99 g, 12.42 mmol) in 58% yield. ^1H NMR (CDCl3, 300.0 MHz) δ (ppm): δ 7.72 (d, *J* = 5.4 Hz, 4H), 7.55 (d, *J* = 5.7 Hz, 2H), 7.44 (s, 2H).

Tetrakis(4'-(2,4-diamino-1,3,5-triazin-6-yl)-[1,1'-biphenyl]-4-yl)methane (4): a mixture of Tetrakis(4'-cyano-[1,1'-biphenyl]-4-yl)methane (3.75 g, 5.18 mmol), dicyandiamide (2.18 g, 25.93 mmol) and KOH (85%, 0.32 g, 4.85 mmol) in methyl cellosolve (25 mL) was stirred at 140 ^oC for 24 h under nitrogen atmosphere. The mixture was then cooled to room temperature and poured into methanol (125 mL). The precipitated solid was filtered, washed with boiling water and methanol, respectively, and dried under vacuum at 90 ^oC to give a white solid (5.05 g, 4.76 mmol) in 92% yield. ^1H NMR (500 MHz, DMSO-d_6) δ (ppm): 8.31 (d, *J* = 7.6 Hz, 2H), 7.78 (dd, *J* = 15.1, 7.7 Hz, 4H), 7.41 (d, *J* = 7.3 Hz, 2H), 6.76 (s, 4H); ^{13}C NMR (500 MHz, DMSO-d_6) δ (ppm): 170.29, 167.87, 146.35, 142.28, 137.58, 136.63, 131.49, 128.78, 126.78, 109.74, 64.36. FTIR (neat, cm^{-1}): 3607, 3469, 3320, 3172, 1599, 1511, 1427, 1381, 1240, 992, 808.

3. Crystallization of the compound HOF-4

Compound **4** (200 mg, 0.189 mmol) was dissolved in DMF (20 mL) under heating. The resulting solution was cooled to room temperature and filtered. The filtrate was divided to 8 small disposable scintillation vials. These vials were allowed to sit and evaporate at room temperature for a week. Colorless needle-like crystals were obtained in 79% yield.

4. Fitting of pure component isotherms

The measured experimental isotherm data for C_2H_4 on HOF-4 were fitted with the dual-Langmuir isotherm model

$$q = q_{A,sat}\frac{b_A p}{1+b_A p} + q_{B,sat}\frac{b_B p}{1+b_B p} \tag{1}$$

with *T*-dependent parameters

$$b_A = b_{A0}\exp\left(\frac{E_A}{RT}\right); \quad b_B = b_{B0}\exp\left(\frac{E_B}{RT}\right)$$

For the pure component isotherms of C_2H_6, a simpler single-site Langmuir model is of adequate accuracy. The fit parameters for both components are specified in Table S2. Figure S7 presents a comparison of the experimentally determined component loadings for C_2H_4, on HOF-4 at 296 K with the isotherm fits using parameters specified in Table S2. The fits are excellent over the entire range of pressures (Note: HOF-4a adsorbs the unsaturated C_2H_4 in preference to the saturated C_2H_6. When all the strong adsorption sites are occupied, further adsorption of C_2H_4 is only possible at weaker sites. Consequently, the isotherms of C_2H_4 exhibit an inflection. To describe such inflection we need a 2-site Langmuir fit. C_2H_6 isotherms do not exhibit any inflection and so a single site Langmuir isotherm is of sufficient accuracy).

5. Calculations of adsorption selectivity

The selectivity of preferential adsorption of component 1 over component 2 in a mixture containing 1 and 2, can be formally defined as

$$S_{ads} = \frac{q_1/q_2}{p_1/p_2} \tag{2}$$

In equation (2), q_1 and q_2 are the component loadings of the adsorbed phase in the mixture. The calculations of S_{ads} are based on the use of the Ideal Adsorbed Solution Theory (IAST) of Myers and Prausnitz.[1]

Based on the IAST calculations for C_2H_4/C_2H_6 adsorption selectivities in HOF-4, at a total pressure of 100 kPa, the value of S_{ads} for HOF-4 is 14. This value is higher than that for MgMOF-74, CoMOF-74, and CuBTC.[2]

6. Isosteric heats of adsorption

The isosteric heat of adsorption, Q_{st}, were calculated using the Clausius-Clapeyron equation by differentiation of the dual-Langmuir fits of the isotherms.

Figure S8 compares the isosteric heats of adsorption, Q_{st}, for C_2H_4 and C_2H_6 in HOF-4. The binding energy for C_2H_4 in HOF-4 is 44 kJ mol^{-1} ; this value is comparable in magnitude to that of MgMOF-74, and CoMOF-74. [2]

7. Simulations of C_2H_4/C_2H_6 breakthroughs in packed beds

Transient breakthrough simulations were carried out using the simulation methodology described in the literature.[3, 4] For the breakthrough simulations, the following parameter values were used: framework density, ρ= 899 kg m^{-3}, length of packed bed, L = 0.12 m; voidage of packed bed, ε= 0.75; superficial gas velocity at inlet, u = 0.00225 m/s. The transient breakthrough are presented in our investigation in terms of a *dimensionless* time, τ, defined by dividing the actual time, t, by the characteristic time, $\frac{L\varepsilon}{u_0}$.

Let us first consider the adsorption phase of the PSA operations. Figure 2d shows transient breakthrough of an equimolar C_2H_4/C_2H_6 mixture in an adsorber bed packed with HOF-4. The inlet gas is maintained at partial pressures $p_1 = p_2 = 50$ kPa. The more poorly adsorbed saturated C_2H_6 breaks through earlier and can be recovered in nearly pure form. From the gas phase concentrations at the exit of the adsorber, we can determine the % C_2H_6; this information is presented in Figure S9. During the adsorption cycle, C_2H_6 at purities > 99% can be recovered for a certain duration of the adsorption cycle.

Once the entire bed is in equilibrium with the partial pressures $p_1 = p_2 = 50$ kPa, the desorption, or "blowdown" cycle is initiated, by applying a vacuum or purging with inert gas. Figure S9b shows % C_2H_4 in the outlet gas of an adsorber bed packed with HOF-4 in the desorption cycle. For production of ethene as feedstock for polymerization purposes, the required purity level is 99.95%+ can be recovered during the time interval indicated by the arrow in Figure S9a.

Notation

b_A	dual-Langmuir constant for species *i* at adsorption site A, Pa^{-1}
b_B	dual-Langmuir constant for species *i* at adsorption site B, Pa^{-1_i}
c_i	molar concentration of species *i* in gas mixture, mol m^{-3}
c_{i0}	molar concentration of species *i* in gas mixture at inlet to adsorber, mol m^{-3}
L	length of packed bed adsorber, m
p_i	partial pressure of species *i* in mixture, Pa
p_t	total system pressure, Pa
q_i	component molar loading of species *i*, mol kg^{-1}
$q_{sat,A}$	saturation loading of site A, mol kg^{-1}
$q_{sat,B}$	saturation loading of site B, mol kg^{-1}
S_{ads}	adsorption selectivity, dimensionless
t	time, s
T	absolute temperature, K
u	superficial gas velocity in packed bed, m s^{-1}

Greek letters

	voidage of packed bed, dimensionless
	framework density, kg m^{-3}
	time, dimensionless

Subscripts

i	referring to component *i*
A	referring to site A
B	referring to site B

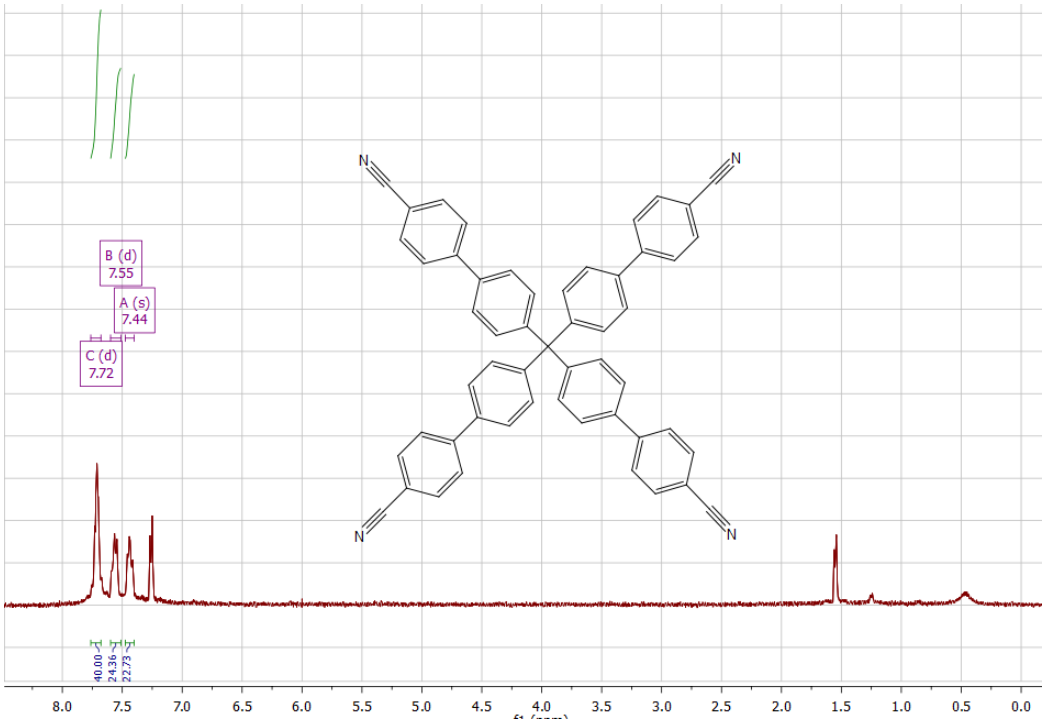

Figure S0. ^{1}H NMR spectra of the organic building block **3**.

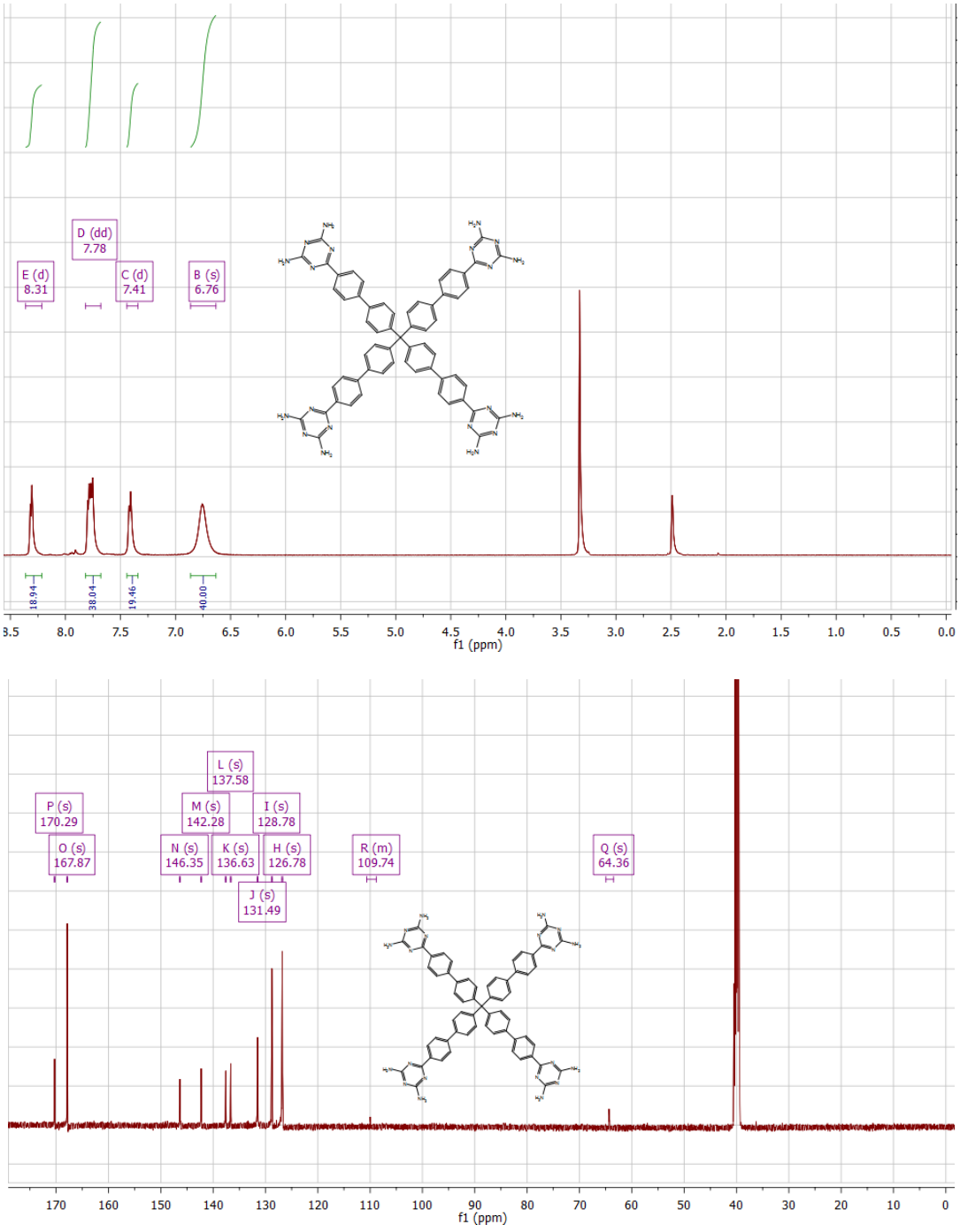

Figure S1. ^{1}H NMR (top) and ^{13}C NMR (bottom) spectra of the activated organic building block **4**.

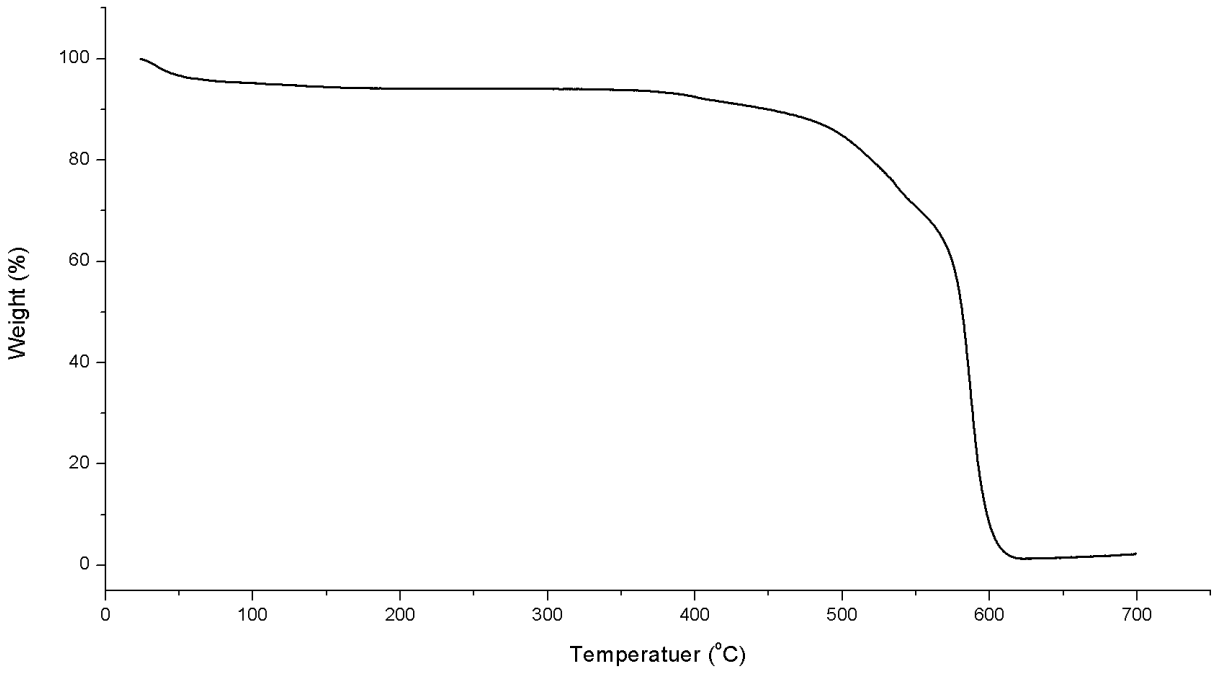

Figure S2. TGA curve of **HOF-4a**.

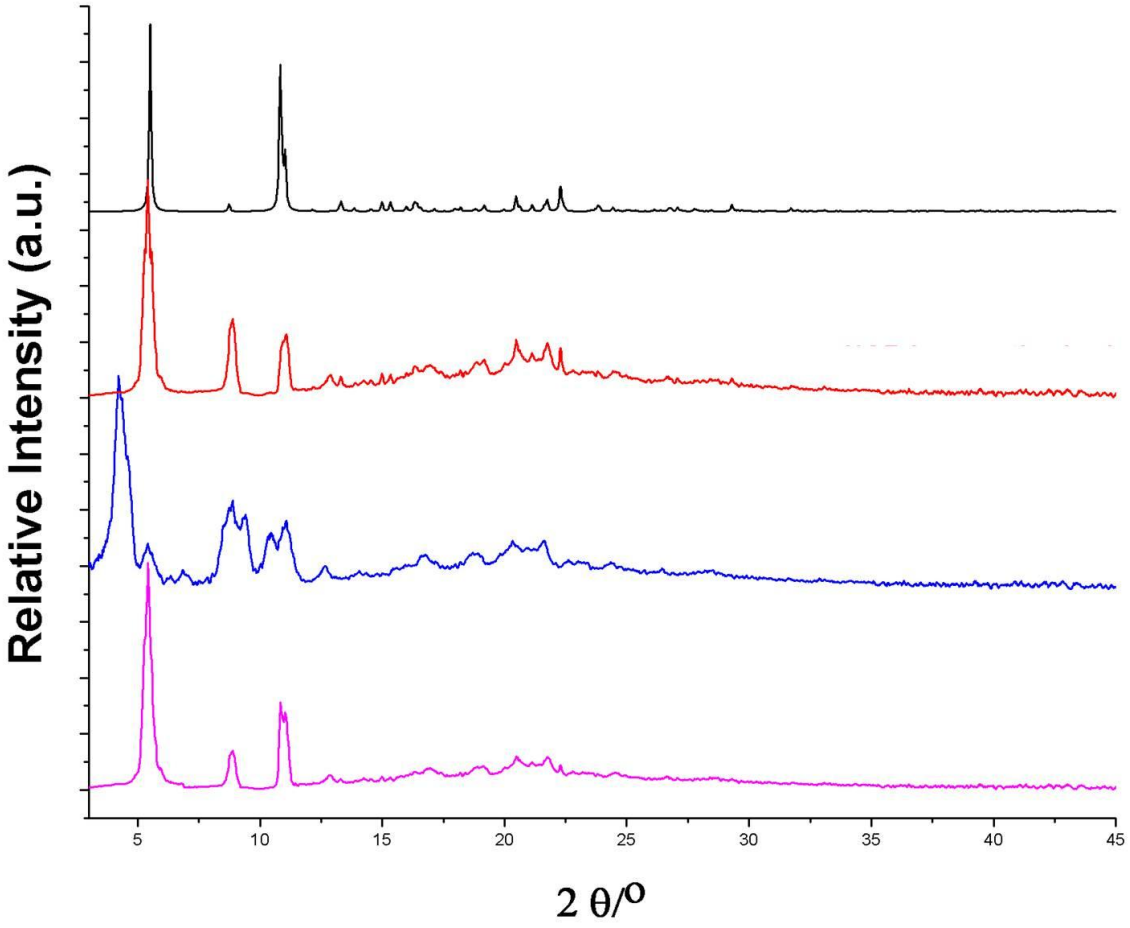

Figure S3. PXRD of simulated **HOF-4** (black), as-synthesized **HOF-4** (red), **HOF-4a** (blue) , and regenerated **HOF-4** (pink)**.**

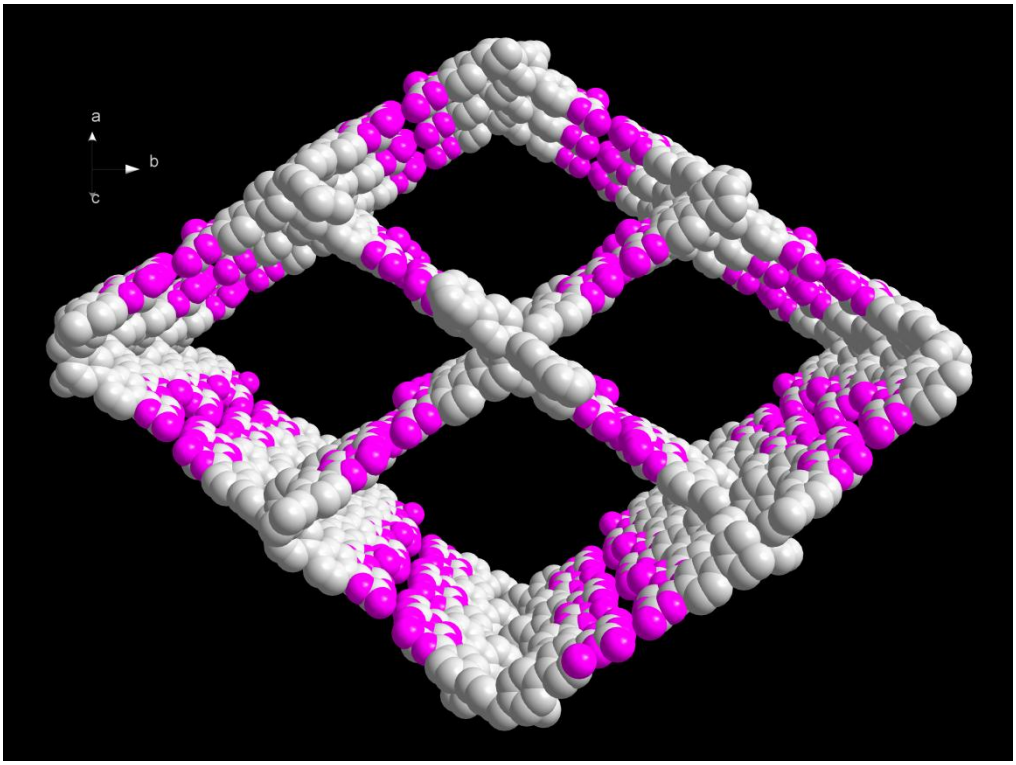

Figure S4. Rhombic channels in the single net of **HOF-4** along [101] direction with an approximate dimension of *c.a.* 40 Å × 30 Å along the diagonals

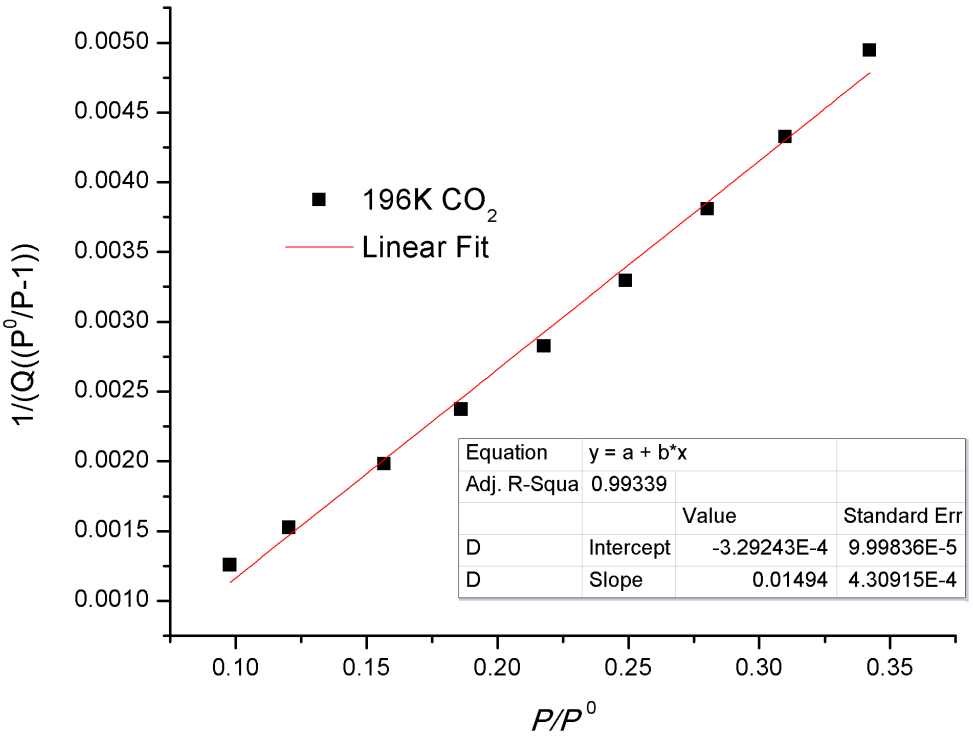

S_{BET} = (1/(-0.00033+0.01494)) / 22414 × 6.023 × 10^{23} × 0.170 × 10^{-18} = 312.67 m^2g^{-1}

Figure S5. CO_2 adsorption isotherm at 196 K (a) and the BET surface areas of **HOF-4a** (b).

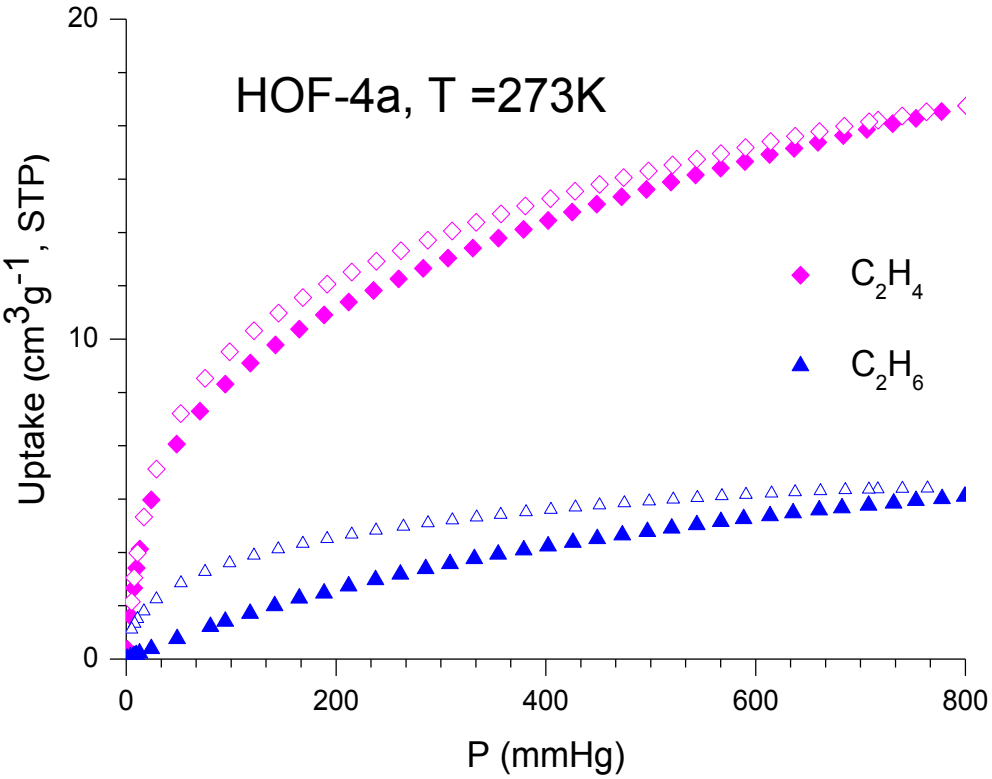

Figure S6. Single-component sorption isotherms for C_2H_4/C_2H_6 in **HOF-4a** at 273 K (Solid symbol: adsorption, open symbol: desorption).

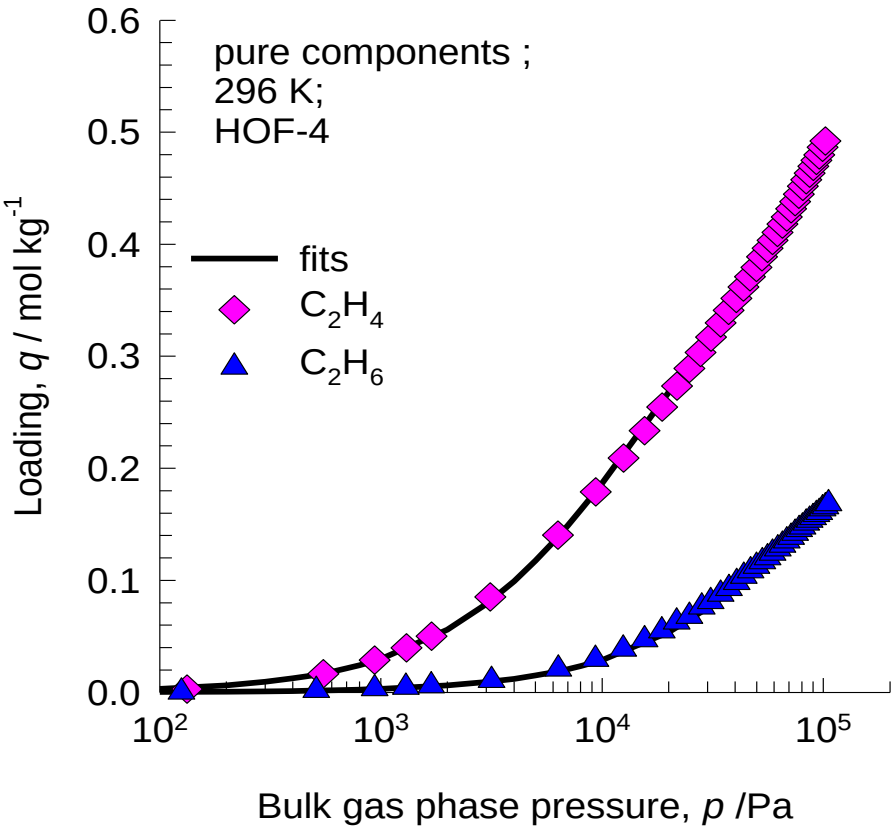

Figure S7. Comparison of the experimentally determined component loadings for C_2H_4, and C_2H_6 in HOF-4 at 296 K with the isotherm fits using parameters specified in Table S2.

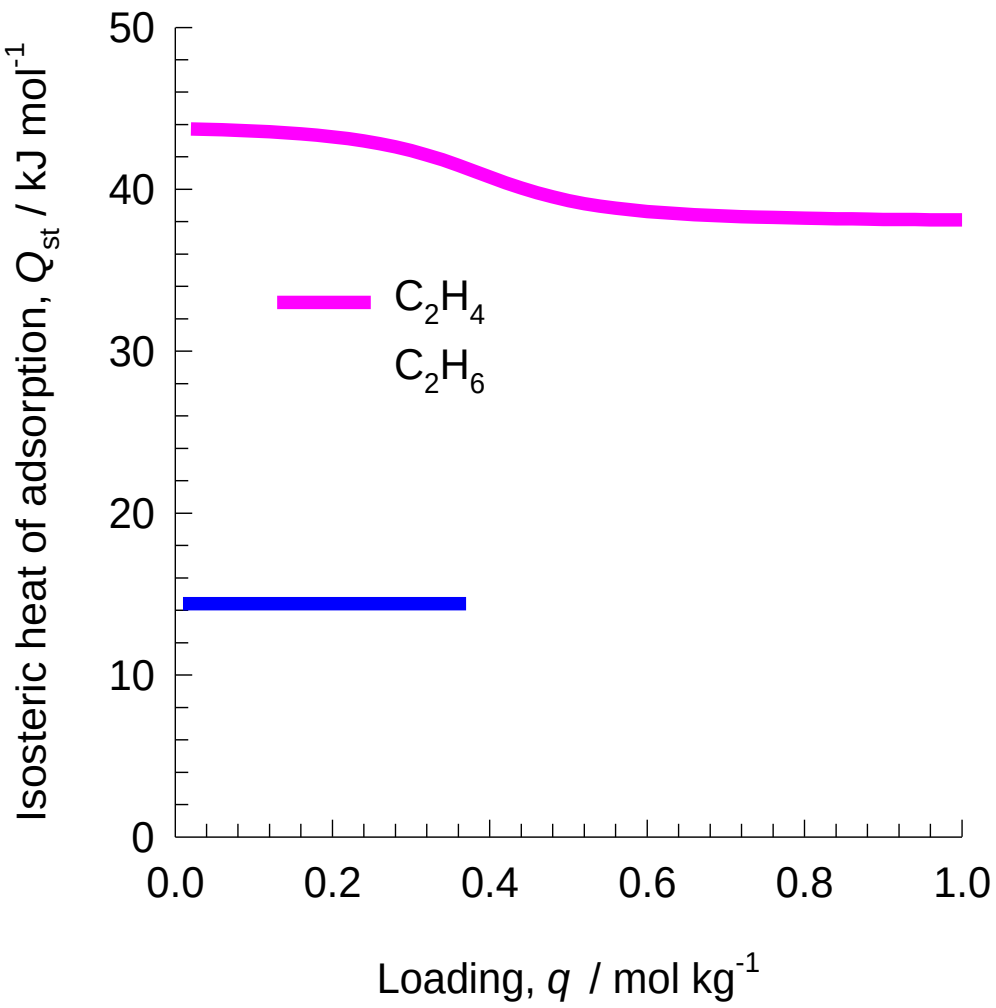

Figure S8. Comparison of the isosteric heats of adsorption, Q_{st}, for C_2H_4, and C_2H_6 in HOF-4.

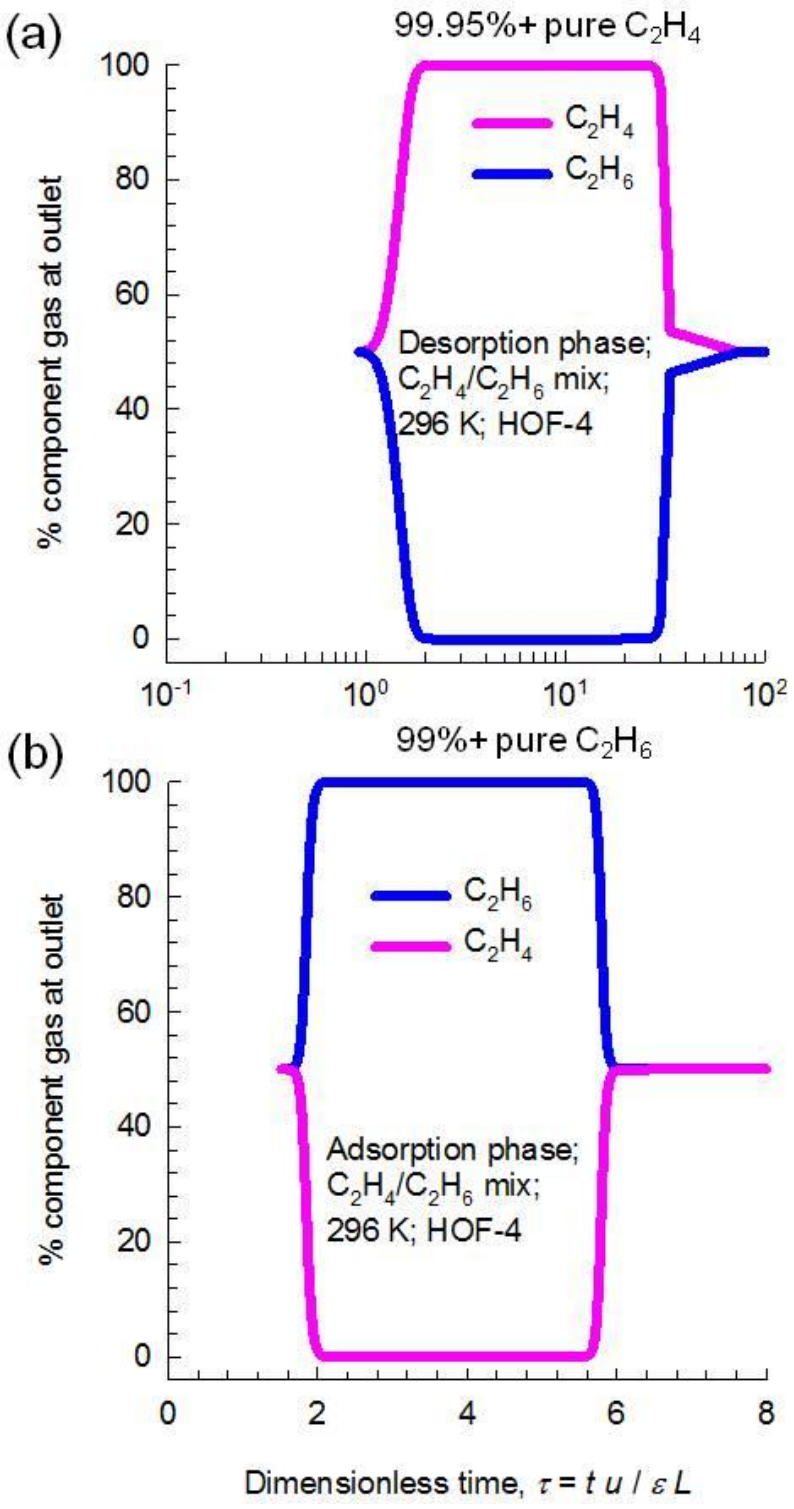

Figure S9. % C_2H_4 and % C_2H_6 in the outlet gas of an adsorber bed packed with HOF-4 in the (a) desorption cycle and (b) adsorption cycle. The inlet gas is maintained at partial pressures $p_1 = p_2$ = 50 kPa, at a temperature of 296 K.

Table S1. Geometry of hydrogen-bonds linked together by adjacent four building blocks in **HOF-4**

D-H…*A*	*D*…H	H…*A*	*D*…*A*	*D*-H…*A*
N5-H5A…N13[i]	0.86	2.1870 (2)	3.0285	166
N10-H10A…N16[ii]	0.86	2.1285(5)	2.9798	170
N14-H14A…N17[iii]	0.86	2.1730(4)	3.0212	169
N15-H15B…N1[ii]	0.86	2.2041(4)	3.0638	179
N19-H19A…N7[i]	0.86	2.1510(4)	2.9390	152
N20-H20A…N12[iv]	0.86	2.0853(4)	2.9407	173

Symmetry codes: (i) = 1/2+x,1-y,1/2+z; (ii) = -1/2+x,1-y,-1/2+z; (iii) = 1/2+x,4-y,-1/2+z;

(iv) = -1/2+x,4-y,1/2+z;

Table S2. Dual-Langmuir fits for C_2H_4, and C_2H_6 in HOF-4. For both components, the fits are based on the adsorption branch of the isotherms.

	Site A			Site B		
	$q_{A,sat}$ mol kg^{-1}	b_{A0} Pa^{-1}	E_A kJ mol^{-1}	$q_{B,sat}$ mol kg^{-1}	b_{B0} Pa^{-1}	E_B kJ mol^{-1}
C_2H_4	2	1.28×10^{-13}	38	0.4	1.32×10^{-12}	44
C_2H_6	0.38	2.37×10^{-8}	14.4			

Table S3. Crystal data and structure refinement for **HOF-4**

Identification code	**HOF-4**
Empirical formula	$C_{61}H_{48}N_{20}$
Formula weight	1061.19
Temperature (K)	193(2)
Crystal system	Monoclinic
Space group	*P*2/n
a (Å)	20.212(6)
b (Å)	7.275(2)
c (Å)	26.666(8)
α (°)	90.00
β (°)	90.606(6)
γ (°)	90.00
Volume ($Å^3$)	3921(2)
Z	2
Calculated density (g/cm^3)	0.899
Adsorption coefficient (mm^{-1})	0.057
F(000)	1108.0
Crystal size (mm)	0.4 × 0.07 × 0.05
Radiation	MoKα (λ = 0.71073)
Theta range for data collection	4.98 to 50.02 °
Index ranges	$-24 \le h \le 24$, $-8 \le k \le 7$, $-31 \le l \le 31$
Reflections collected	20646
Independent reflections	6927 [R_{int} = 0.0549, R_{sigma} = 0.0570]
Data/restraints/parameters	6927/0/393
Goodness-of-fit on F^2	1.133
Final R indexes [$I >= 2\sigma(I)$]	R_1 = 0.0976, wR_2 = 0.1992
Final R indexes [all data]	R_1 = 0.1442, wR_2 = 0.2139
Largest diff. peak/hole (e. $Å^{-3}$)	0.50/-0.42
CCDC No.	1010353

8. References

[1] A. L. Myers and J. M. Prausnitz, *A.I.Ch.E.J.*, 1965, **11**, 121-130.

[2] Y. He, R. Krishna, B. Chen, *Energy Environ. Sci.*, 2012**, 5**, 9107.

[3] R. Krishna and J. R. Long, *J. Phys. Chem. C*, 2011, **115**, 12941-12950.

[4] R. Krishna, *Microporous Mesoporous Mater.*, 2014, **185**, 30-50.